www.czasopisma.pan.pl PAN POLSKA AKADEMIA NAUK www.journals.pan.pl

Arch. Metall. Mater., Vol. 61 (2016), No 3, p. 1447–1452

DOI: 10.1515/amm-2016-0237

A. LISIŃSKA-CZEKAJ*,#, M. RERAK*, D. CZEKAJ*, M. LUBINA*, B. GARBARZ-GLOS**, W. BĄK***

LOW TEMPERATURE BROAD BAND DIELECTRIC SPECTROSCOPY OF MULTIFERROIC $Bi_6Fe_2Ti_3O_{18}$ CERAMICS

In the present research the tool of broadband dielectric spectroscopy was utilized to characterize dielectric behavior of $Bi_6Fe_2Ti_3O_{18}$ (BFTO) Aurivillius-type multiferroic ceramics. Dielectric response of BFTO ceramics was studied in the frequency domain ($\Delta\nu$=0.1Hz – 10MHz) within the temperature range ΔT=-100°C – 200°C. The Kramers-Kronig data validation test was employed to validate the impedance data measurements and it was found that the measured impedance data exhibited good quality justifying further analysis. The residuals were found to be less than 1%, whereas the "chi-square" parameter was within the range $\chi^2 \sim 10^{-7}$-10^{-5}. Experimental data were analyzed using the circle fit of simple impedance arc plotted in the complex Z"-Z' plane (Nyquist plot). The total ac conductivity of the grain boundaries was thus revealed and the activation energy of ac conductivity for the grain boundaries was calculated. It was found that activation energy of ac conductivity of grain boundaries changes from E_A=0.20eV to E_A=0.55eV while temperature rises from T=-100°C up to T=200°C. On the base of maxima of the impedance semicircles ($\omega_m\tau_m$=1) the relaxation phenomena were characterized in terms of the temperature dependence of relaxation times and relevant activation energy was calculated (E_A=0.55eV).

1. Introduction

Dielectric spectroscopy [1] has gained tremendous increase in popularity in the recent years. A great strength of this method is that, with appropriate data analysis, it is often possible to characterize the different electrically active regions in a material, investigate the dynamics of bound or mobile charge in the bulk or interfacial regions of any kind of solid or liquid material [2]. Now it is a frequently used tool employed to analyze the electrical properties of a wide variety of electroceramics, including ferroelectrics, solid electrolytes and mixed conductors [3].

Aurivillius phases of $Bi_4Ti_3O_{12}$-$BiFeO_3$ (BFTO) system have attracted widespread scientific interest due to the possibility of rich functionality of BFTO-based novel materials. BFTO materials are known to combine ferroelectric, semiconducting and ferromagnetic properties [4] and are recognized as prospective multiferroics [5, 6]. As far as multiferroic materials promise an important practical applications in spintronics, BFTO-based compounds are potentially attractive for producing high-performance ceramics for information processing, and information storage applications [6, 7, 8].

Among the different ferromagnetic compounds of BFTO system $Bi_6Fe_2Ti_3O_{18}$ was found to be interesting because of the high dielectric transition temperature (T=805°C) and quadratic magnetoelectric nature [7, 9]. Although several researches on $Bi_6Fe_2Ti_3O_{18}$ ceramics have already been performed either by us [e.g. 6, 10, 11] or other scientific groups [e.g. 12, 13, 14] the low temperature dielectric behavior of BFTO was not studied yet. Therefore the present research was focused on study of dielectric response of $Bi_6Fe_2Ti_3O_{18}$ – the Aurivillius structure multiferroic ceramics in the frequency domain at low temperature.

2. Experimental

The mixed oxide method was employed for fabrication of $Bi_6Fe_2Ti_3O_{18}$ ceramics. First homogeneous stoichiometric mixture of initial powders was prepared. After that green compacts were formed and subjected to calcination at T_{calc}=720°C. The calcined compacts were powdered and the pellets were formed and pressed into disks with the diameter of 10mm and 1mm thickness. Final densification of $Bi_6Fe_2Ti_3O_{18}$ ceramics was reached by pressureless sintering at temperature T_s=850°C for t_s=3h. The samples exhibited orthorhombic symmetry of *Fmm2* (42) space group. For electrical measurements both surfaces of the disk-shaped ceramic samples were polished and silver paste electrodes were deposited on both surfaces.

Dielectric properties of BFTO ceramics were studied with an analyzer (Alpha-A High Performance Frequency Analyzer system) combined with cryogenic temperature control system (Quatro Cryosystem). The temperature measuring range was ΔT=-100 – 200°C, and the frequency range was $\Delta\nu$=0.1Hz – 10MHz. The measurements were performed in nitrogen atmosphere over the heating cycles. Spectra were collected at programmed temperatures with the temperature step size ΔT=10°C after 15 min of temperature stabilization. Impedance

* UNIVERSITY OF SILESIA, INSTITUTE OF TECHNOLOGY AND MECHATRONICS, 12, ZYTNIA STR., 41-200 SOSNOWIEC, POLAND

** PEDAGOGICAL UNIVERSITY, INSTITUTE OF ENGINEERING, 2, PODCHORĄŻYCH STR., 30-084 KRAKÓW, POLAND

*** PEDAGOGICAL UNIVERSITY, INSTITUTE OF PHYSICS, 2 PODCHORĄŻYCH STR., 30-084 KRAKÓW, POLAND

Corresponding author: agata.lisinska-czekaj@us.edu.pl

at every frequency (40 measuring points per decade were registered) was measured until consistency was achieved. The WinDETA Novocontrol software was used for the data manipulation. The Kramers-Kronig data validation test was employed in the impedance data analysis [2, 15]. Quality of the broadband dielectric measurements was estimated according to the following methods: "pseudo χ-squared" value (χ^2) and relative differences, between the data and its K-K-compliant fit (residuals: $\Delta_{Re,i}$ and $\Delta_{Im,i}$) [2, 15]. Impedance spectra were analyzed by means of non-linear least-squares fitting [16].

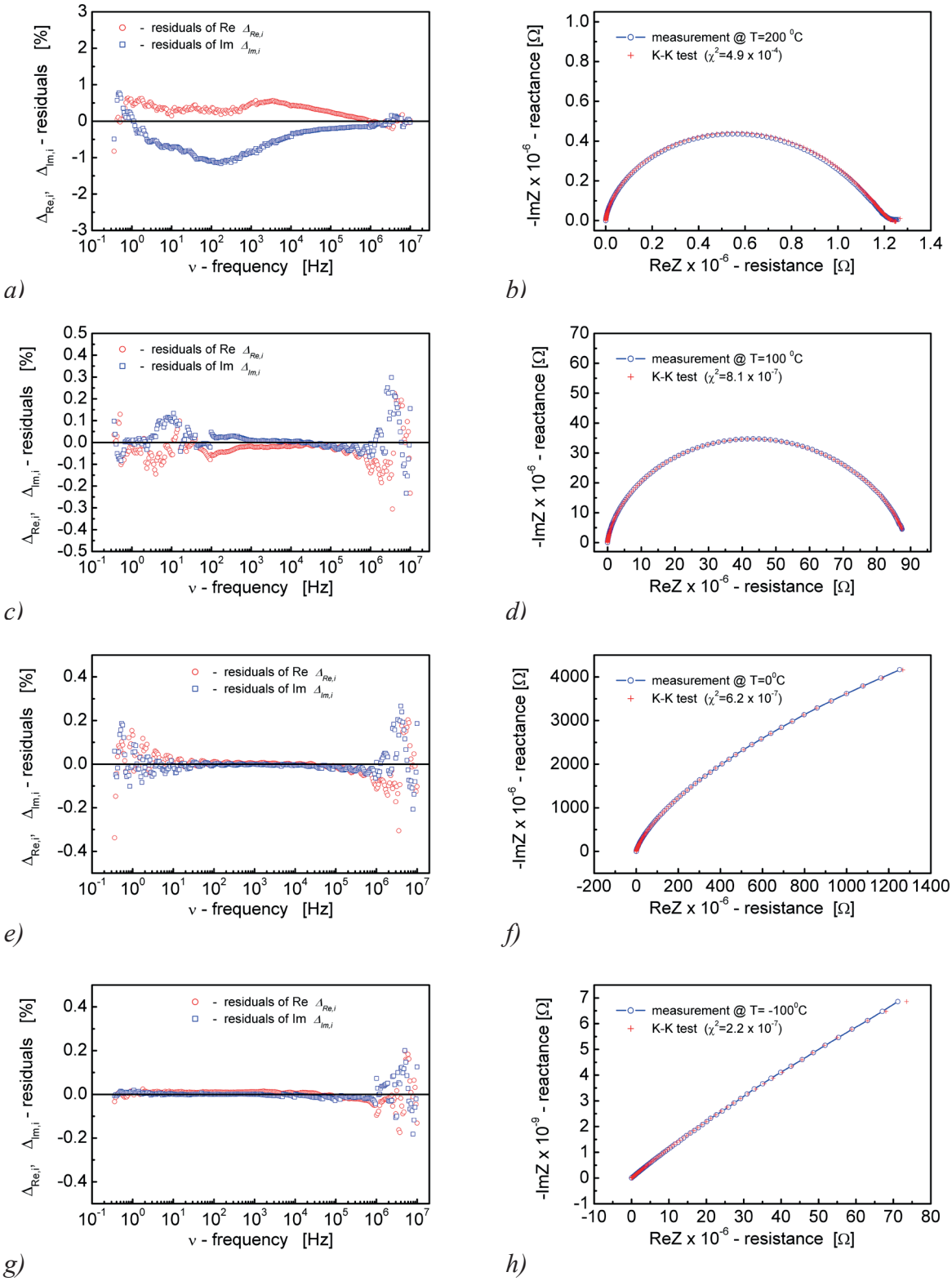

Fig. 1. Kramers – Kronig transform test results of impedance data (a, c, e, g) and impedance diagram with K-K transform test result (b, d, f, h) for $Bi_6Fe_2Ti_3O_{18}$ ceramics measured at temperature T=200°C (a, b), T=100°C (c, d), T=0°C (e, f), T=-100°C (g, h)

3. Results and discussion

Data validation. Knowing the quality of the measured impedance data is essential for a proper analysis. In that connection the Kramers – Kronig (K-K) relations, which are based on the principle of casuality, present a very useful tool for data validation [2, 15]. A data set that complies with the K-K transformation rules must be: (i) casual, (ii) a linear response, (iii) stable, and (iv) finite for all frequencies. The Kramers – Kronig rule states that the imaginary part of a dispersion is completely determined by the form of the real part of dispersion over the frequency range $\infty \geq \nu \geq 0$. Similarly the reall part is determined by the imaginary dispersion form [2]. Practical application of the impedance data validation method in the study of Aurivillius-type electroceramics was described by us in details elsewhere [e.g., 17].

The calculations necessary for performing the K-K test were accomplished with a computer program by B.A. Boukamp [2, 15]. The results obtained are shown in Fig. 1. As an example the relative difference plots (residuals) for BTFO ceramics studied at temperature within the range ΔT=(200 – -100)°C are shown in Fig. 1*a*, *c*, *e*, *g*, where the red circles present the real part differences and the blue squares the imaginary part differences.

The impedance diagram in a complex plane -*Z*' vs. Z' (blue circles) combined with results of the K-K test (red crosses) for the measurements carried out at the relevant temperatures are presented in Fig. 1*b*, *d*, *f*, *h*. In his connection it should be pointed out that for KK-compliant data only a noise distribution around the frequency axis should be observed. A clear trace around the frequency axis indicates that the data is corrupted [2, 15].

One can see in Fig. 1a that the data recorded at temperature T=200°C are corrupted by non steady state behavior. However in that case the deviation from K-K behavior is quite small (residuals are less than 1%). Visual inspection of the results given in Fig. 1*b* show a very good agreement between the measurement (blue circles) and K-K calculations (red crosses). Also an obtained value of the "chi-squared" parameter is χ^2=4.9×10^{-5}.

In case of the lower temperatures (Fig. 1*c*, *e*, *g*) the residuals are less than 0.5% and frequency regions of high instability are ν<10Hz and ν>1MHz. The quality parameter "chi-squared" reached value of χ^2=8.1×10^{-7} – 2.2×10^{-7} for temperature going down to T=-100°C. The above mentioned proved high quality of the measurements and fully justified that the further analysis of the impedance data was reasonable.

Analysis of the impedance data. In an ideal case, the results of impedance spectroscopy measurements over a wide range of frequencies can be presented by semicircles in a complex *Z''-Z'* plane (Nyquist plot). Each semicircle represents the contribution of a particular process (electrodes and contacts, grain boundaries, grains interior) to the total impedance of the sample. Measured values in the form of Nyquist plots are rarely ideal semicircles (Fig. 2). They are often described as depressed and/or deformed semicircles, with their centre lying below the *x*-axis. This phenomenon, called non-Debye relaxation, is attributed to the distribution of Debye relaxations with different time constants. Possible explanations for a non-Debye relaxation behavior of grain boundaries are: (i) inhomogeneity and variations among the grain boundaries combined in series/parallel connection, (ii) it is intrinsic to the measured response of each individual grain boundary and (iii) it is a combination of the former reasons [18].

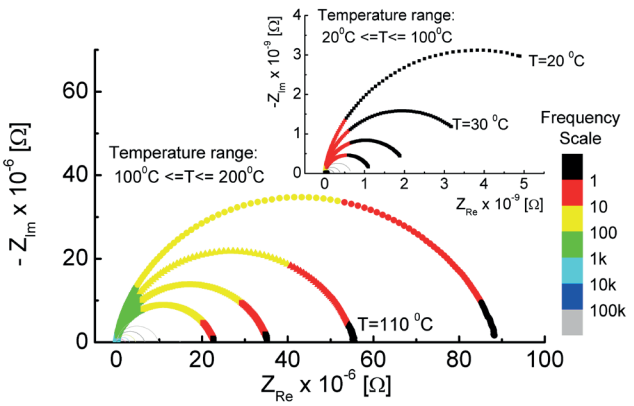

Fig. 2. Comparison of impedance spectra plotted in *Z''-Z'* plane for ΔT=20 -200 °C

Distribution of relaxations with different time constants may be mathematically expressed by the Cole-Cole equation:

$$Z = Z_{\mathrm{Re}} + jZ_{\mathrm{Im}} = R_G + \frac{R_{GB}}{1+\left(j\omega R_{GB}C\right)^{(1-\alpha)}} \qquad (1)$$

where Z is the overall impedance, Z_{Re}, and Z_{Im} are the real and imaginary components of the impedance, R_G is the resistance of the grain interior, R_{GB} is the resistance of the grain boundary region, α is a constant, while C represents the capacitance of the grain boundary region. Parameter α is related to the depression angle β by the equation $\alpha=\beta/(\pi/2)$. Meaning of all the parameters and/or variables of the equation (1) is shown in Fig. 3.

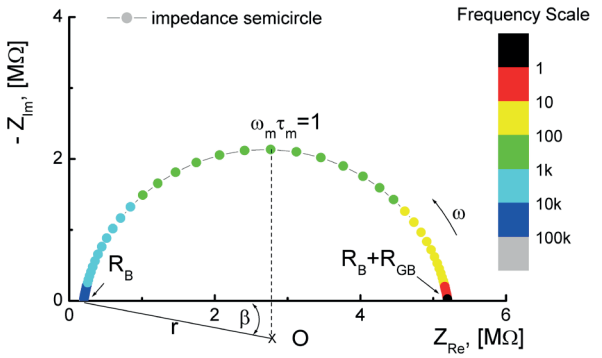

Fig. 3. Impedance plane plot for a depressed circular arc; β- depression angle. Meaning of all the parameters is illustrated

Fig. 4 and Fig. 5 show the impedance spectra for BFTO ceramics in a form of Nyquist plots. The spectra were measured within temperature range ΔT=200°C - -100°C. From the visual inspection of IS data one can see that the complex plot (Fig. 4a) is in a form of one depressed semicircle (depression angle β=19°) with a large radius, starting from the origin, reaching a maximum at a frequency w_{max}=53992 rad/s, making an

intercept on the real axis at Z_{Re}=1.2x10^6 W and exhibiting a small tail at low frequencies (ν <1 Hz). With a decrease in temperature the low frequency tail disappeared (Fig. 4b), radius and intercept on the real axis increased (Z_{Re}=8.8x10^7 Ω), whereas the depression angle (β) and the frequency (ω_{max}) decreased (β=13.5°, ω_{max}=81 rad/s).

a)

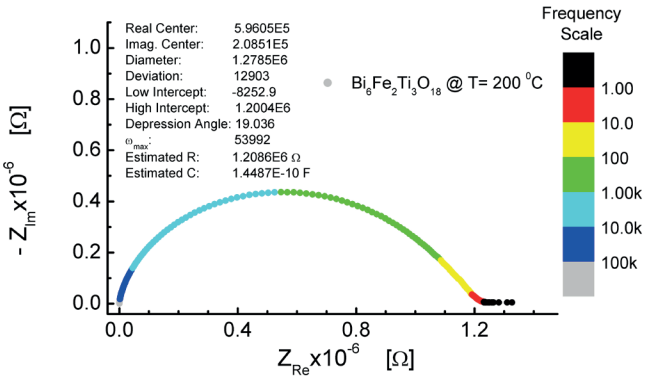

b)

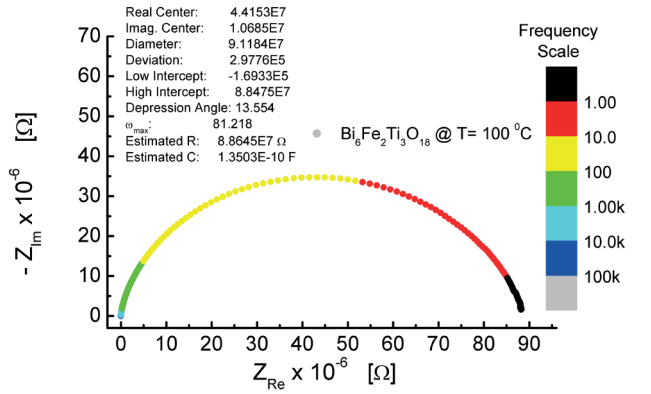

Fig. 4. Impedance diagrams in the complex Z''-Z' plane measured for $Bi_6Fe_2Ti_3O_{18}$ ceramics at temperature T=200°C (a) and T=100°C (b)

The lower the temperature the stronger were the changes of the circular arc parameters (Fig. 5a). Within the temperature range ΔT=-10°C – -100°C the impedance spectra resembled only a very beginning part of a semicircle (Fig. 5b). They started from the beginning of the coordinate system Z'' – Z' and did not reach an intercept with the real axis of impedance Z'.

a)

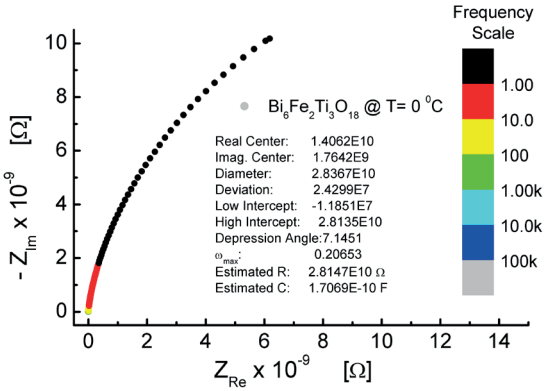

b)

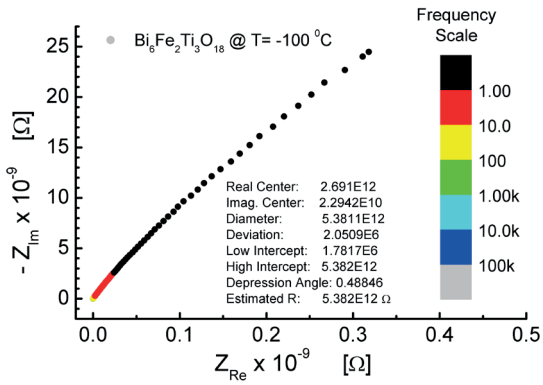

Fig. 5. Impedance diagrams in the complex Z''-Z' plane measured for $Bi_6Fe_2Ti_3O_{18}$ ceramics at temperature T=0°C (a), T=-100°C (b); isotropic (a) and free scale (b) was used for data presentation

On the base of the circle fit (Fig. 3) of the impedance data, performed with non-linear least-squares fitting method [16], resistance of the grain boundaries was estimated at every point within the temperature domain (ΔT=-100°C – 200°C) with a step size of ΔT=10°C. Thus ac conductivity was calculated and results are given in Fig. 6 in a ln-1000/T scale, where T is temperature in Kelvin.

One can see in Fig. 6 that estimated conductivity of grain boundaries exhibited non-linear dependence within the whole temperature range. However, two linear regions (with a linear fit quality parameter R_0=0.998 and R_0=0.996 for T≥0°C and T≤-10°C, respectively) were revealed. Activation energy was calculated and it was found that activation energy of ac conductivity of grain boundaries changes from E_A=0.199eV to E_A=0.553eV while temperature rises from T=-100°C up to T=200°C.

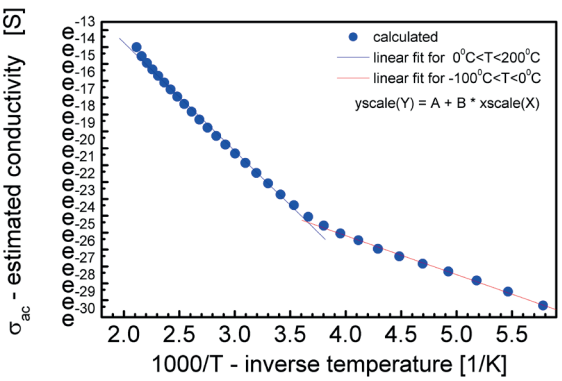

Fig. 6. Dependence of estimated conductivity of grain boundaries of $Bi_6Fe_2Ti_3O_{18}$ ceramics on inverse absolute temperature

The impedance data was also used to calculate the relaxation time of the electrical phenomena in the $Bi_6Fe_2Ti_3O_{18}$ ceramics using the relation τ=1/ω=1/2$\pi\nu$, where ν is the relaxation frequency. The nature of the variation of relaxation time (τ) of the grain boundary with the reciprocal of temperature (1/T) is shown in Fig. 7 for the $Bi_6Fe_2Ti_3O_{18}$ ceramics. The activation energy in the relaxation process was determined by the temperature dependent relaxation time

constant τ which obeys the Arrhenius law in the following equation:

$$\tau = \tau_0 \exp\left(\frac{E_A}{kT}\right) \quad (2)$$

where E_A is the activation energy involved in the dielectric relaxation process, τ_0 is the pre-exponential factor, k is the Boltzmann constant, and T is the absolute temperature.

The activation energy for relaxations on grain boundaries was evaluated from the slope of lnτ against 1000/T curve (parameter of the linear fitting R_0=0.999), and was found to be E_A=0.553eV. The pre-exponential factor was also calculated $\tau_0=3.5\times10^{-10}$s, so the ν_0 (i.e. a phonon frequency in terms of ac hopping conductivity [19]), was estimated ν_0=453MHz.

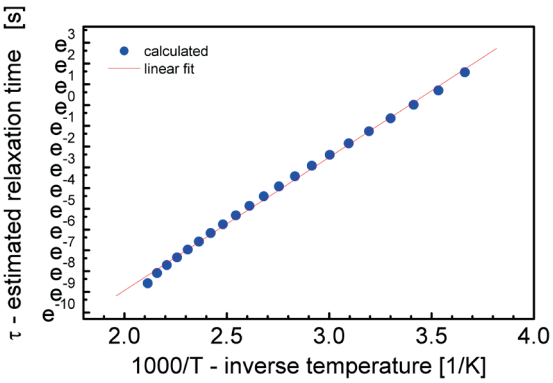

Fig. 7. Dependence of the grain boundary relaxation time on inverse temperature

4. Conclusions

Analysis from the impedance formalism proved that influence of grain boundaries was predominant in $Bi_6Fe_2Ti_3O_{18}$ ceramics due to the presence of distributed relaxation times originating from different grain boundary combinations. The relaxation times were decreasing with the rise in the measuring temperature suggesting that the net relaxation phenomena is associated with the charge carrier transport mechanism. The calculated activation energy, in the high-temperature (i.e. $T\geq0$°C; E_A=0.553eV) regime was attributed to the excitation of the charge carriers from a set of shallow traps and/or oxygen vacancies present at an average depth of 0.5-0.6 eV from the bottom of the conduction band. On the other hand, activation energy calculated in the low-temperature (i.e. $T\leq$-10°C; E_A=0.199eV) regime, suggests different mechanism of ac conductivity. Low values of conductivity activation energy (E_A=0.2-0.45 eV) are typical for protonic conductors. However, a high concentration of oxygen vacancies is necessary for formation of protonic defects leading to the material with protonic conductivity and the Authors realize that the problem requires further studies.

Acknowledgements

The present research was supported by University of Silesia in Katowice, Poland from the funds for science – research potential (NO 1S-0800-001-1-05-01).

REFERENCES

[1] E. Barsoukov, J.R. Macdonald (Eds), Impedance Spectroscopy, Theory, Experiment, and Applications, second ed., John Wiley & Sons, 2005.

[2] B.A. Boukamp, Electrochemical impedance spectroscopy in solid state ionics: recent advances, Solid State Ionics **169**, 65–73 (2004).

[3] E.J. Abram, D.C. Sinclair, A.R. West, A Strategy for Analysis and Modelling of Impedance Spectroscopy Data of Electroceramics: Doped Lanthanum Gallate, Journal of Electroceramics **10** ,165–177(2003).

[4] N.A. Lomanova, M.I. Morozov, V.L. Ugolkov, V.V. Gusarov, Properties of Aurivillius phases in the $Bi_4Ti_3O_{12}$ - $BiFeO_3$ system, Inorg. Mater. **42**, 189 – 195 (2006).

[5] W. Erenstein, N.D. Mathur, J.F. Scott, Mutiferroic and magnetoelectric materials, Nature **442**, 759-65 (2006).

[6] A. Lisińska-Czekaj, Wielofunkcyjne materiały ceramiczne na osnowie tytanianu bizmutu, Wydawnictwo Gnome, Uniwersytet Śląski, Katowice 2012.

[7] E. Jartych, M. Mazurek, A. Lisińska-Czekaj, D. Czekaj, Hyperfine interactions in some Aurivillius $Bi_{m+1}Ti_3Fe_{m-3}O_{3m+3}$ compounds, Journal of Magnetism and Magnetic Materials **322**, 51–55 (2010).

[8] A. Lisińska–Czekaj, D. Czekaj, Ferroelektryki o warstwowej strukturze perowskitopodobnej BWPT. W: Z. Surowiak (Red.) Elektroceramika ferroelektryczna, Wydawnictwo Uniwersytetu Śląskiego, 105-162, Katowice (2004).

[9] E. Jartych, K.Gąska, J. Przewoźnik, Cz. Kapusta, A. Lisińska-Czekaj, D. Czekaj, Z. Surowiec, Hyperfine interactions and irreversible magnetic behavior in multiferroic Aurivillius compounds, Nukleonika **58**, 1 47−51 (2013).

[10] A. Lisińska–Czekaj, Fabrication of $Bi_6Fe_2Ti_3O_{18}$ ceramics by mixed oxide method, Materials Science Forum **730-732**, 100-104 (2013).

[11] A. Lisińska–Czekaj, D. Czekaj, Characterization of $Bi_6Fe_2Ti_3O_{18}$ ceramics with impedance spectroscopy, Materials Science Forum **730-732**, 76-81(2013).

[12] K. Srinivas, P. Sarah, S.V. Suryanarayana, Impedance spectroscopy study of polycrystalline $Bi_6Fe_2Ti_3O_{18}$, Bulletin of Materials Science **26**, 2 ,247–253(2003).

[13] D. Zientara, M. Bućko, J. Polnar, Synthesis of $Bi_6Fe_2Ti_3O1_8$ Aurivillius phase by wet chemical methods, Advances in Science and Technology **67**, 164-169 (2010).

[14] M. Bućko, J. Polnar, J. Przewoźnik, J. Żukrowski Cz. Kapusta, Magnetic properties of the $Bi_6Fe_2Ti_3O_{18}$ Aurivillius phase prepared by hydrothermal method, Advances in Science and Technology **67**, 170-175 (2010.

[15] B.A. Boukamp, A linear Kronig-Kramers transform test for immitance data validation, J. Electrochem. Soc. 142 (1995) 1885-1894.

[16] D. Czekaj, A. Lisinska-Czekaj, T. Orkisz, J. Orkisz, G. Smalarz, Impedance spectroscopic studies of sol–gel derived barium strontium titanate thin films, Journal of the European Ceramic Society **30**, 465–470 (2010).

[17] H. Bernard, A. Lisinska-Czekaj, J. Dzik, K. Osinska, D. Czekaj, Fabrication, structural and ac impedance studies of layer–structured $Bi_4Ti_3O_{12}$ ceramics, Archives of Metallurgy and Materials **56**, 4, 1137-1148 (2011).

[18] G. Brankovic, Z. Brankovic, V.D. Jovic, J.A. Varela, Fractal

approach to ac impedance spectroscopy studies of ceramic materials, Journal of Electroceramics **7**, 89-94 (2001).

[19] A. Osak, J. Piwowarczyk, Studies of the dc and ac hopping electrical conductivity in ferroelectric $Pb(Fe_{1/3}Sb_{2/3})_xTi_yZr_zO_3$, Technical Transactions. Fundamental Sciences, 1-NP 59-75 (2011).